THE JOURNAL OF BIOLOGICAL CHEMISTRY VOL. 286, NO. 38, pp. 32948–32961, September 23, 2011

The Assembly of Proline-rich Membrane Anchor (PRiMA)-linked Acetylcholinesterase Enzyme

GLYCOSYLATION IS REQUIRED FOR ENZYMATIC ACTIVITY BUT NOT FOR OLIGOMERIZATION[*][S]

Received for publication, May 16, 2011, and in revised form, July 14, 2011 Published, JBC Papers in Press, July 27, 2011, DOI 10.1074/jbc.M111.261248

Vicky P. Chen, Roy C. Y. Choi, Wallace K. B. Chan, K. Wing Leung, Ava J. Y. Guo, Gallant K. L. Chan, Wilson K. W. Luk, and Karl W. K. Tsim[1]

From the Division of Life Science and Center for Chinese Medicine, The Hong Kong University of Science and Technology, Clear Water Bay Road, Hong Kong SAR, China

Acetylcholinesterase (AChE) anchors onto cell membranes by a transmembrane protein PRiMA (proline-rich membrane anchor) as a tetrameric form in vertebrate brain. The assembly of AChE tetramer with PRiMA requires the C-terminal "t-peptide" in AChE catalytic subunit ($AChE_T$). Although mature AChE is well known *N*-glycosylated, the role of glycosylation in forming the physiologically active PRiMA-linked AChE tetramer has not been studied. Here, several lines of evidence indicate that the *N*-linked glycosylation of $AChE_T$ plays a major role for acquisition of AChE full enzymatic activity but does not affect its oligomerization. The expression of the $AChE_T$ mutant, in which all *N*-glycosylation sites were deleted, together with PRiMA in HEK293T cells produced a glycan-depleted PRiMA-linked AChE tetramer but with a much higher K_m value as compared with the wild type. This glycan-depleted enzyme was assembled in endoplasmic reticulum but was not transported to Golgi apparatus or plasma membrane.

Acetylcholinesterase (AChE),[2] a heavily *N*-glycosylated enzyme, is responsible for the hydrolysis of acetylcholine at the cholinergic synapses, which is essential for the control of neurotransmission. In vertebrates, AChE possesses alternative C-terminal R or H or T peptide that defines its post-translational maturation, quaternary association, and anchoring (1). $AChE_R$ generates soluble monomers (G_1), $AChE_H$ generates glycolipid-anchored dimers (G_2), and $AChE_T$, which is largely predominant in the brain and muscle, generates a multitude of oligomers. The functional localization of $AChE_T$ depends on the association of tetramer(s) with anchoring proteins: the collagen tail (ColQ) and the proline-rich membrane anchor (PRiMA). The ColQ-associated AChE (A_{12}) is attached to the basal lamina at vertebrate neuromuscular junctions (2, 3), and the PRiMA-linked AChE tetramer (G_4) is anchored on cell membrane of the brain (4–6) and muscle (7). The association of the catalytic subunits ($AChE_T$) with ColQ and PRiMA proteins is mostly based on a tight interaction between the four C-terminal t-peptides of $AChE_T$ subunits and a proline-rich attachment domain that exists in both ColQ and PRiMA (8, 9).

N-Glycosylation, a form of co-translational or post-translational modification, occurs in a very large proportion of secreted or membrane-bound proteins; pre-assembled carbohydrate chains are co-translationally attached to asparagines and may be post-translationally modified in the endoplasmic reticulum (ER) and in the Golgi apparatus, resulting in chains of various sizes, composition, and complexity. The glycans can affect a host of cellular processes. In vertebrates, AChE molecules were shown to have various numbers of carbohydrate chains. Different glycosylation patterns of AChE have been found in different tissues and in different molecular forms. In human and bovine, G_2 AChE from erythrocyte membrane is more heavily glycosylated than G_4 AChE in the brain (10, 11). In chicken, AChE from muscle is ~5 kDa heavier than the enzyme from brain, possibly due to variation of glycosylation (12). In bovine muscle, G_4 AChE carries carbohydrate chains of the complex type, whereas G_1 appears to possess only the high mannose type (13). These lines of evidence suggest that different post-translational modifications in the carbohydrate chains affect the oligomerization of AChE molecular forms.

Without added oligosaccharides, many proteins remain misfolded, aggregated, and degraded without a proper transportation from ER to the Golgi complex and beyond (14). The *N*-glycosylation of human $AChE_T$ plays an important function during the biosynthesis and secretion of G_1 and G_2 forms of AChE in transfected cells; the elimination of *N*-glycosylation sites in $AChE_T$ mutants dramatically reduced the secreted enzyme (15). Post-translational modification of *N*-glycans was used as a marker for the progression of AChE through the different subcellular compartments in cultured muscles (16). In addition, the accumulation of molecular forms of AChE with an altered pattern of glycosylation has been observed in the brain and cerebrospinal fluid of Alzheimer patients (17). In particular, AChE is associated with the senile plaques and shows a higher degree of glycosylation than in normal tissues (18).

* This work was supported by grants from the Research Grants Council of Hong Kong (662407, 660409, 662911, F-HK21/06T) and the Croucher Foundation (CAS-CF07/08.SC03) (to K. W. K. T. and R. C. Y. C.).

[S] The on-line version of this article (available at http://www.jbc.org) contains supplemental Figs. 1–4.

[1] To whom correspondence should be addressed. Tel.: 852-2358-7332; Fax: 852-2358-1559; E-mail: botsim@ust.hk.

[2] The abbreviations used are: AChE, acetylcholinesterase; $cAChE_T$, chicken $AChE_T$; PRiMA, proline-rich membrane anchor; ColQ, collagen tail; Endo H, endoglycosidase H; ER, endoplasmic reticulum; GM130, Golgi matrix protein 130; PM, plasma membrane; PNGase F, peptide N-glycosidase F; ATCh, acetylthiocholine iodide; iso-OMPA, tetraisopropylpyrophosphoramide; ER, endoplasmic reticulum.

Here we analyzed the role of *N*-glycosylation on the assembly and trafficking of PRiMA-linked G_4 AChE. By expressing $AChE_T$ mutants, in which single or multiple *N*-glycosylation sites were removed, we found that *N*-glycans play important roles for AChE biosynthesis. The depletion of *N*-glycosylation did not prevent the assembly of $AChE_T$ subunits with PRiMA in forming a PRiMA-linked G_4 tetramer. However, the glycan-depleted PRiMA-linked AChE, which was retained in the ER compartment, was enzymatically less active and stable than that of wild-type G_4 AChE. These results suggest that in addition to assisting the folding of $AChE_T$ protein, the *N*-glycans are essential for the proper trafficking of PRiMA-linked AChE from ER to Golgi apparatus.

EXPERIMENTAL PROCEDURES

Cell Cultures—The human embryonic kidney fibroblast cell line (HEK293T) was obtained from the American Type Culture Collection (Manassas, VA). Cells were cultured in Dulbecco's modified Eagle's medium supplemented with 10% fetal bovine serum at 37 °C in a water-saturated 5% CO_2 incubator. All reagents for cell cultures were purchased from Invitrogen.

DNA Constructs and Transfection—The cDNAs encoding wild-type human $AChE_T$ and glycosylation mutants ($AChE_T^{N296Q}$, $AChE_T^{N381Q}$, $AChE_T^{N495Q}$, and $AChE_T^{N296Q/N381Q/N495Q}$, as described in Ref. 15) were subcloned in a pcDNA4 vector under a CMV promoter. The cDNA encoding full-length mouse PRiMA, tagged with an HA epitope (YPY DVP DYA) at the C terminus, was subcloned in a pEF-BOS vector under the control of an EF-1α promoter (4, 19). The cDNA encoding full-length chicken $AChE_T$ was subcloned in a pcDNA3 vector under a CMV promoter (20, 21). One day after plating, cultured HZK293T cells were transfected with cDNAs by calcium phosphate precipitation (22). The cells were collected 2 days after the transfection in a low salt lysis buffer (10 mM HEPES, pH 7.5, 1 mM EDTA, 1 mM EGTA, 150 mM NaCl, and 0.5% Triton X-100) with the addition of the following protease inhibitors: 10 μg/ml leupeptin, 10 μg/ml aprotinin, 20 μM pepstatin, and 2.5 mM benzamidine HCl. The homogenization was done by vortexing for 15 min, and the homogenates were clarified by centrifugation for 30 min at 16,000 $\times$ *g* at 4 °C.

Sucrose Density Gradients—Separation of AChE molecular forms was performed by sucrose density gradient analysis as described previously (6, 22). In brief, continuous sucrose gradients (5–20%) in a detergent-containing buffer (10 mM HEPES, pH 7.5, 1 mM EDTA, 1 mM EGTA, 0.2% Brij-97, and 150 mM NaCl) were prepared in 12-ml polyallomer ultracentrifugation tubes with a 0.4-ml cushion of 60% sucrose at the bottom. Samples of cell extracts (0.2 ml) containing equal amounts of protein were mixed with the sedimentation markers, alkaline phosphatase (6.1 S; Roche Applied Science) and β-galactosidase (16 S; Roche Applied Science) and loaded onto the gradients to be centrifuged at 38,000 rpm in a Sorvall TH 641 rotor at 4 °C for 16 h. Approximately 45 fractions were collected and subjected to enzymatic activity assays.

Enzymatic Activity Assay—AChE activity was determined according to the method of Ellman (23) with minor modifications. The cell lysates were incubated with 0.1 mM tetraisopropylpyrophosphoramide (iso-OMPA; Sigma) for 10 min to inhibit butyrylcholinesterase activity. Samples of about 5–20 μl were then added to the reaction mixture with final concentrations of 0.625 mM acetylthiocholine iodide (ATCh; Sigma) and 0.5 mM 5,5′-dithiobis-2-nitrobenzoic acid (Sigma) in 80 mM sodium phosphate, pH 7.4. The increase in absorbance at 410 nm was recorded, and the specific enzyme activity was expressed as absorbance units/min/μg of protein. The effects of substrate concentration on AChE activities were determined under similar assay conditions using increasing ATCh concentrations. K_m values were obtained from Lineweaver-Burk plots. The amounts of the various AChE forms were determined by summation of the enzymatic activities corresponding to the peaks of their respective sedimentation profiles. The sedimentation values of the enzymes were calculated from the positions of the markers, alkaline phosphatase and β-galactosidase, as described previously (22).

Western Blot Analysis—For non-reducing SDS-PAGE, G_2 fractions obtained from the sucrose density gradients were denatured at 100 °C for 5 min in a buffer containing 2% SDS and separated by electrophoresis in 8% SDS-PAGE. For reducing SDS-PAGE, the protein lysate was denatured in the presence of 2% SDS and 100 mM β-mercaptoethanol. Anti-human AChE antibody E-19 (1:2,000, Santa Cruz Biotechnology, Santa Cruz, CA) (24), anti-chicken AChE antibody 3D10 (1:5,000, purified at 1 mg/ml) (12), or anti-tubulin antibody (1:50,000, Sigma) (25) was used for Western blot analyses. The immune complexes were visualized using the enhanced chemiluminescence (ECL) method (Amersham Biosciences) in strictly standardized conditions. The intensities of the bands were quantified by ImageJ 1.43u analysis software using a calibration plot constructed from a parallel gel with serial dilutions of $AChE_T$-expressed cell lysates. The labeling intensities of protein bands were in the non-saturating range of calibration curves.

De-glycosylation—Ninety μl of cell lysate, obtained from the transfected cell cultures, were mixed with 10 μl of 10$\times$ incubation buffer (200 mM sodium phosphate, pH 6, 100 mM EDTA,1% SDS, 10% β-mercaptoethanol, and 5% Triton X-100). One mM PMSF was added to inhibit protease activity. The reaction was incubated with 0.5 μl of endoglycosidase H (Endo H; Roche Applied Science) or peptide N-glycosidase F (PNGase F; Roche Applied Science) for 16 h at 37 °C and then processed for Western blot analysis. For de-glycosylation without sample denaturation, SDS and β-mercaptoethanol were excluded from 10$\times$ incubation buffer. The experiment was performed without PMSF to preserve AChE enzymatic activity. The reaction was incubated with 2 μl of Endo H or PNGase F for 24 h at 37 °C and then processed for other assays.

Subcellular Fractionation—Forty-eight hours after the transfection, the cultured HEK293T cells, grown in 100-mm dishes, were detached from confluent cultures in 0.5 ml of homogenization buffer (10 mM HEPES, pH 7.4, 1 mM EDTA, 0. 25 M sucrose, supplemented with protease inhibitors as in the low salt lysis buffer). The cells were disrupted using 10 strokes in a Dounce homogenizer on ice followed by 10 passages through a 30-gauge needle with a 1-ml syringe. Nuclei and unbroken cells were pelleted by centrifugation at 500 $\times$ *g* for 10 min. The clarification process was repeated one or more times until no visible pellet was detected. Post-nuclear supernatants from the

centrifugation steps were combined and centrifuged at 80,000 × *g* for 1 h. The vesicle pellet was resuspended in 0.8 ml of homogenization buffer and applied on top of linear iodixanol gradients (1–20%, Sigma). The gradients were centrifuged in a Sorvall TH 641 rotor at 200,000 × *g* for 3 h at 4 °C. Sequential 1-ml fractions were collected from the top of the gradient, and the distribution of the intracellular markers was examined by Western blotting with different antibodies: calnexin (1:10,000, Sigma) (26) for the ER, Golgi matrix protein 130 (GM130) (1:1,000, BD Biosciences) (27) for the Golgi apparatus, and Na^+/K^+-ATPase (1:1,000, Abcam, Cambridge, UK) (28) for the plasma membrane (PM).

Immunoprecipitation—Five hundred μl of G_2 or G_4 fractions, obtained from the sucrose density gradients, were incubated with anti-human AChE antibody E-19 (1:200) or anti-chicken AChE monoclonal antibody (3D10, 1:200) at 4 °C overnight. Neither antibody cross-reacted with the other corresponding antigen (21). Each sample was added with 30 μl of protein G-agarose (Roche Applied Science) and incubated for 4 h at 4 °C. The protein G beads were centrifuged in a microcentrifuge tube and washed three times with ice-cold extraction buffer. The supernatant was discarded by careful aspiration, and the protein G beads were then subjected to Western blotting and probed with anti-human AChE and anti-chicken AChE antibodies.

Immunofluorescence Analysis—The transfected HEK293T cell cultures were fixed by 4% paraformaldehyde in PBS for 10 min followed by 50 mM ammonium chloride (NH_4Cl) treatment for 30 min. Samples were blocked by 5% BSA in PBS with or without 0.2% Triton X-100 for 1 h at room temperature. Cultures were stained with anti-human AChE antibody (1:500) or double-stained with anti-chicken AChE (1:500) and anti-human AChE (1:500) antibodies for 16 h at 4 °C followed by the corresponding fluorescence-conjugated secondary antibodies (Alexa 488-conjugated anti-goat. Alexa 555-conjugated anti-mouse) for 2 h at room temperature. Samples were dehydrated serially with ice-cold 50, 75, 95, and 100% ethanol and mounted with fluorescence mounting medium (DAKO, Carpinteria, CA). The samples were then examined using a fluorescence microscopy (DMIRE2, Leica, Wetzlar, Germany). Images were captured by Leica confocal software (Version 2.61) using PL APO 40 × 0.75 DRY objective with excitation at 488 nm/emission at 500–535 nm for green and excitation at 543 nm/emission at 560–620 nm for red.

Other Assays—Protein concentrations were measured by the Bradford method with a kit from Bio-Rad. Statistical tests were performed using one-way analysis of variance; differences from basal or control values were classified as * where $p < 0.05$, ** where $p < 0.01$, and *** where $p < 0.001$.

RESULTS

Glycosylation of $AChE_T$—To demonstrate that $AChE_T$ is post-translationally *N*-glycosylated in our expression system of HEK293T cells, we used two glycosidases: Endo H and PNGase F. Endo H cleaves only high mannose glycan chains that have not been modified in the Golgi apparatus, whereas PNGase F removes modified complex chains that have been processed in the Golgi apparatus (Fig. 1*A*). As reported by Velan (15), the wild-type human $AChE_T$ ($AChE_T^{WT}$) sequence possesses three putative *N*-linked glycosylation sites, located at 296, 381, and 495 (Fig. 1*B*). We used mutants in which these sites were suppressed by replacing asparagines by glutamines to determine whether they are all actually utilized in the glycosylation of $AChE_T$. Each site was suppressed individually in $AChE_T^{N296Q}$, $AChE_T^{N381Q}$, and $AChE_T^{N495Q}$ mutants. Additionally, a triple mutant, $AChE_T^{N296Q/N381Q/N495Q}$, devoid of all three *N*-glycosylation sites, was constructed. The cDNAs encoding $AChE_T^{WT}$, $AChE_T^{N296Q}$, $AChE_T^{N381Q}$, $AChE_T^{N495Q}$, and $AChE_T^{N296Q/N381Q/N495Q}$ were separately transfected in HEK293T cells.

In $AChE_T^{WT}$ cDNA-transfected cells, G_1/G_2 form AChE was formed (supplemental Fig. 1). The cell lysates were incubated with Endo H or PNGase F, and the digested proteins were compared by Western blotting; there were at least two species of $AChE_T$ migrating on the gel at 68~70 kDa (Fig. 1*C*). The two species of $AChE_T$ were shifted to a single band after digestion with Endo H or PNGase F, producing a single band of low molecular size (~60 kDa) corresponding to the de-glycosylated $AChE_T$. The formation of AChE molecular forms (*i.e.* G_1/G_2) by the glycosylation mutants was similar to that of the wild type (supplemental Fig. 1). For the glycosylation mutants, different migration patterns of these mutants were observed; double bands of $AChE_T$ appeared in $AChE_T^{N296Q}$- and $AChE_T^{N495Q}$-transfected cells but only a single band occurred in $AChE_T^{N381Q}$-transfected cells (Fig. 1*C*). In addition, the molecular mass of $AChE_T^{N296Q/N381Q/N495Q}$ was at ~60 kDa (the lowest band), corresponding exactly to totally un-glycosylated $AChE_T$. The protein sizes formed by these mutants were in line with the previous study (15). The elimination of glycosylation by Endo H or PNGase F treatment resulted in a decrease in apparent molecular mass of $AChE_T$ to ~60 kDa for all the mutants (Fig. 1*C*). Therefore, the three putative *N*-linked glycosylation sites of $AChE_T$ are fully utilized, and $AChE_T$ contains no other *N*-glycosylation site.

The cDNA encoding $AChE_T$ or the glycosylation mutants was transfected together with PRiMA cDNA into HEK293T cells: G_4 AChE was formed in all cases (supplemental Fig. 1). In the co-expression of $AChE_T^{WT}$ and PRiMA, additional species of $AChE_T$ with higher apparent masses of 68 ~ 72 kDa were revealed (Fig. 2*A*, *upper panel*). In contrast, the co-expression of PRiMA had no significant effect on the glycosylation pattern of the mutants (Fig. 2*A*, *upper panel*).

By comparing the protein expression of $AChE_T^{WT}$ and its glycosylation mutants in transfected HEK293T cells, we then examined the role of PRiMA in directing the expression profile of $AChE_T$. The expression levels of $AChE_T^{WT}$ and its mutants in the absence of PRiMA were comparable, differing by less than 10% (Fig. 2*A*, *lower panel*). Co-expression of $AChE_T$ with PRiMA markedly increased the protein levels of wild-type and single mutants, except for the $AChE_T^{N296Q/N381Q/N495Q}$ mutant, which remained at a low level of expression (Fig. 2*A*, *lower panel*). In addition, the enzymatic activity of $AChE_T^{WT}$ and its glycosylation mutants in transfected HEK293T cells was compared. In the presence of PRiMA the enzymatic activity was markedly enhanced in all cases, as normalized to $AChE_T$ protein in each sample (Fig. 2*B*); the increase was more obvious in

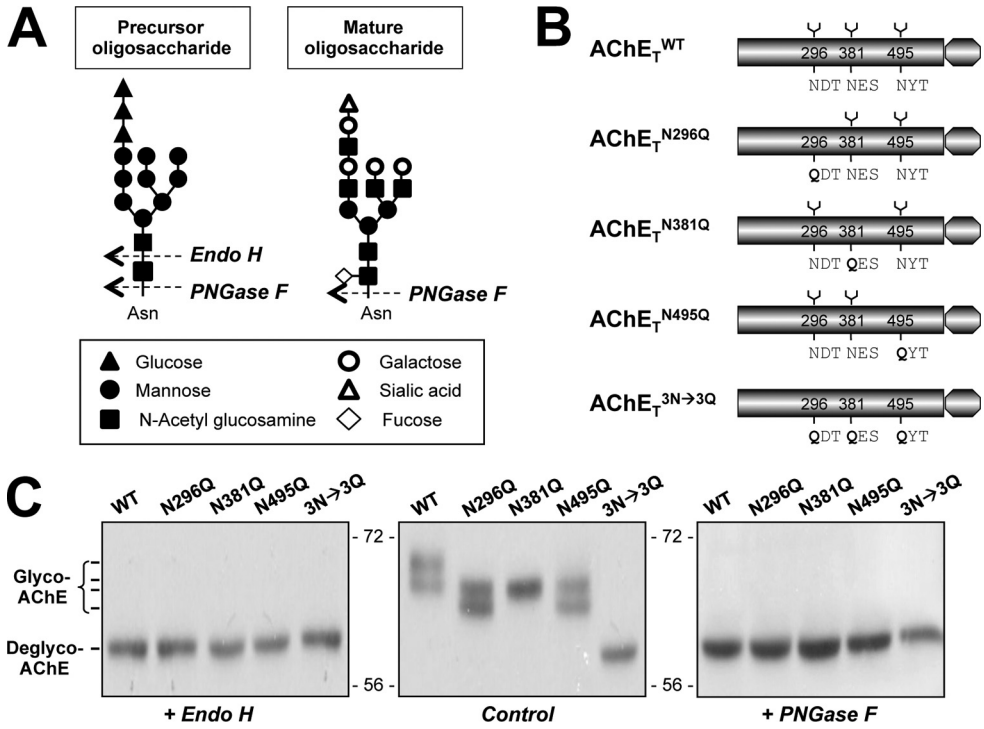

FIGURE 1. **Characterization of *N*-glycosylation of human AChE$_T$.** *A*, representative cutting sites of Endo H and PNGase F are shown. *N*-Linked oligosaccharide chains share a chitobiose core (two *N*-acetyl glucosamine) linked to one side to an asparagine residue of a potential *N*-glycosylation site (Asn-*X*-Ser/Thr) and on the other side to a trimannosyl core (three mannose) that is linked to high mannose structure in precursor oligosaccharide or various complex sugar chains in mature oligosaccharide. Endo H specifically recognizes high mannose oligosaccharides, cleaving between the N-acetylglucosamine residues of the diacetylchitobiose core, whereas PNGase F cleaves all *N*-linked glycans attached to asparagine. A possible example is shown for illustration. *B*, shown are schematic representations of human AChE$_T$ and its glycosylation site mutants. *C*, HEK293T cells were single-transfected with cDNAs encoding AChE$_T^{WT}$, AChE$_T^{N296Q}$, AChE$_T^{N381Q}$, AChE$_T^{N495Q}$, and AChE$_T^{N296Q/N381Q/N495Q}$. The cell lysates were incubated with Endo H or PNGase F and analyzed by Western blotting with anti-AChE antibody. Representative gels from three independent experiments are shown ($n = 3$).

AChE$_T^{WT}$. On the other hand, the enzymatic activity of the glycosylation mutants was dramatically decreased as compared with that of AChE$_T^{WT}$. In the absence of PRiMA, the enzymatic activity of AChE$_T^{N296Q}$ and AChE$_T^{N495Q}$ was reduced to 70 ~ 80% that of AChE$_T^{WT}$, whereas the enzymatic activity of AChE$_T^{N381Q}$ and AChE$_T^{N296Q/N381Q/N495Q}$ was dramatically reduced to only ~10% of the control (Fig. 2*B*). The co-expression with PRiMA did not help that much in terms of AChE activity of those mutants. The rates of hydrolysis of ATCh by AChE$_T^{WT}$ and AChE$_T^{N296Q/N381Q/N495Q}$ were measured as a function of ATCh concentration by using AChE$_T^{WT}$ or AChE$_T^{N296Q/N381Q/N495Q}$ and PRiMA-co-expressed cell lysates (Fig. 2*C*). AChE$_T^{WT}$ exhibited the classical bell-shaped curve of hydrolysis rate *versus* substrate concentration in which the substrate inhibition started from 1 mM of ATCh. On the other hand, AChE$_T^{N296Q/N381Q/N495Q}$ showed no inhibition even at a substrate concentration as high as 3 mM. These results suggest a possible collaboration of the three glycosylation sites in directing AChE folding and/or catalytic activity.

We compared the catalytic properties of AChE$_T^{WT}$ and of its glycosylation mutants. Table 1 shows different K_m values of those mutated enzymes. In general, the PRiMA-linked AChE (*i.e.* G_4) showed a lower K_m as compared with that of G_1/G_2 enzyme (no PRiMA). The K_m values of AChE$_T^{N296Q}$ and AChE$_T^{N495Q}$ enzymes were 15~30% higher than that of AChE$_T^{WT}$ enzyme, and those of AChE$_T^{N381Q}$ and AChE$_T^{N296Q/N381Q/N495Q}$ enzymes were about 60-fold higher. These data suggest that *N*-glycans, particularly on Asn-381, are very important for maintaining the conformation of catalytically active AChE. Differences in K_m appear to contribute to the activity differences as shown in Fig. 2*B*. The Lineweaver-Burk plots for the K_m value determination were shown in supplemental Fig. 2.

In the co-expression of AChE$_T$ and PRiMA, several species of AChE$_T$ migrating on the gel from 68 ~ 72 kDa were revealed; the higher molecular mass species were distinct as compared with that of singly AChE$_T$-expressed cells (Fig. 3*A*, *upper panel*). After treatment with Endo H, the 68~70-kDa bands were shifted to a single band at ~60 kDa, whereas the migration of the highest molecular mass bands at 70~72 kDa was unaffected. Treatment with PNGase F resulted in a mobility shift of all AChE$_T$, producing the completely deglycosylated species at ~60 kDa (Fig. 3*A*, upper *panel*). These results suggested that an extensive glycosylation with more complex sugar chains was triggered in PRiMA-linked G_4 AChE after it was processed from ER to Golgi. In addition, AChE$_T$ was 100% Endo H-sensitive when expressed alone (Fig. 3*A*, *lower panel*) and, therefore, appeared to be retained in the ER; this evidence was also revealed in PRiMA knock-out mice (29). However, AChE$_T$ was only partially Endo H-sensitive when co-expressed with PRiMA, suggesting that a portion of PRiMA-linked G_4 AChE was transported to the Golgi apparatus, as it contained a mixture of high mannose chains and complex oligosaccharides. In that case, a quantification of the Western blotting indicated

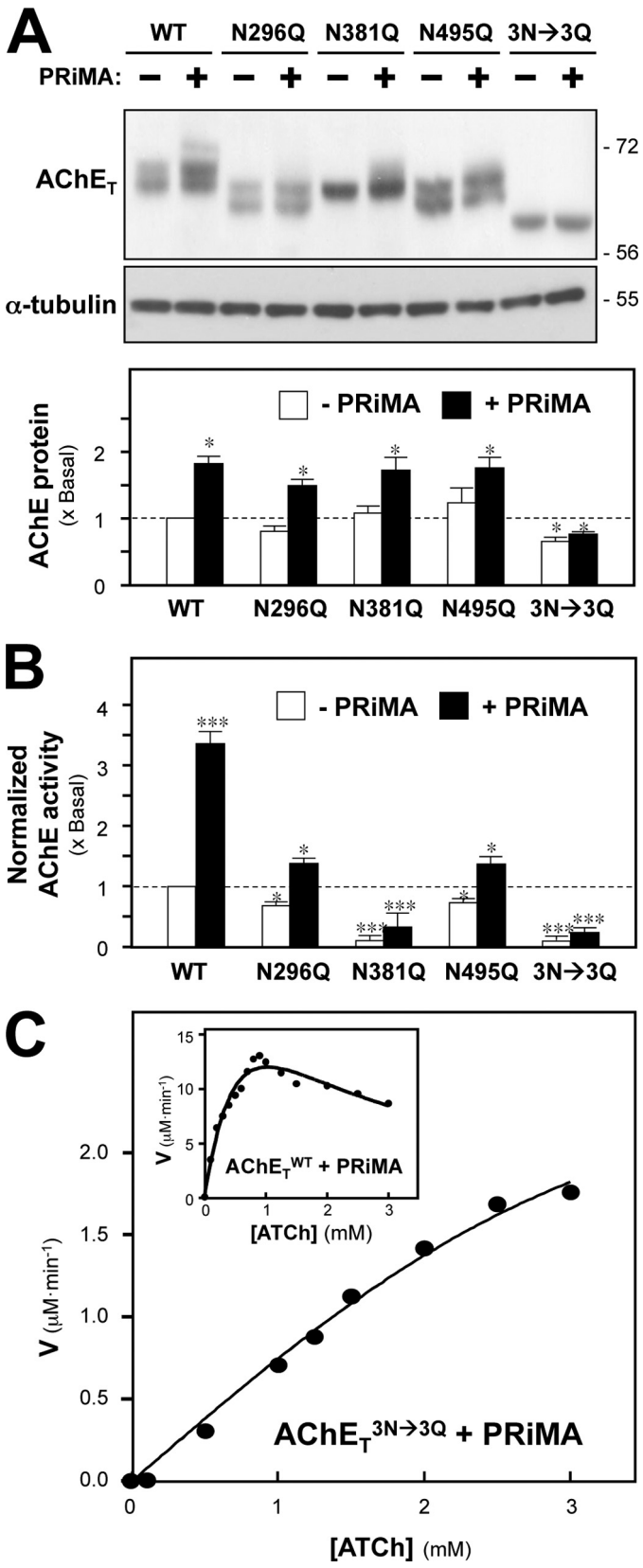

FIGURE 2. ***N*-Glycosylation of AChE$_T$ affects the production of catalytic activity.** *A*, HEK293T cells were transfected with cDNAs encoding AChE$_T^{WT}$, AChE$_T^{N296Q}$, AChE$_T^{N381Q}$, AChE$_T^{N495Q}$, and AChE$_T^{N296Q/N381Q/N495Q}$ with or without PRiMA. The proteins were analyzed as in Fig. 1*C*. α-Tubulin (~55 kDa) served as a loading control. The *lower panel* shows quantitation of AChE$_T$ protein from the blots by calibrated densitometry. *B*, AChE enzymatic activity in the transfected cells from *A* was determined by the Ellman assay. The data are normalized to the amount of AChE$_T$ protein and are expressed as the ratio to the value obtained for cells expressing AChE$_T^{WT}$ alone, which is arbitrarily set to 1. A similar profile was achieved if the enzymatic activity was normalized to total protein (not shown for clarity). *C*, AChE$_T^{WT}$ and PRiMA (*inset*) or AChE$_T^{N296Q/N381Q/N495Q}$ and PRiMA co-expressed cell lysates were subjected to Ellman assay using different concentrations of ATCh substrate. The reaction velocity (*V*) was calculated at each concentration of substrate. Representative profiles from six independent experiments are shown. Values are the means ± S.E. obtained in four independent experiments ($n = 4$), each with triplicate samples. *, $p < 0.05$; ***, $p < 0.001$ compared with AChE$_T^{WT}$ alone control.

TABLE 1

***N*-Glycosylation affects the catalytic function of AChE**

Cell lysates from HEK293T cells expressing AChE$_T^{WT}$, AChE$_T^{N296Q}$, AChE$_T^{N381Q}$, AChE$_T^{N495Q}$, or AChE$_T^{N296Q/N381Q/N495Q}$ with (mainly G_4) or without (mainly G_1/G_2) PRiMA were subjected to Ellman assays using different concentrations of ATCh as substrate, which would not cause substrate inhibition on AChE. The reaction velocity was determined at each concentration of substrate. K_m values were determined according to a Lineweaver-Burk plot. Values are the means ± S.E. obtained from nine independent experiments ($n = 9$).

	−PRiMA	+PRiMA
	μM	μM
AChE$_T^{WT}$	294 ± 82	261 ± 73
AChE$_T^{N296Q}$	326 ± 98	330 ± 69
AChE$_T^{N381Q}$	17,379 ± 2961	16,480 ± 3690
AChE$_T^{N495Q}$	314 ± 71	307 ± 94
AChE$_T^{N296Q/N381Q/N495Q}$	19,058 ± 3667	17,013 ± 2799

that about 70% G_4 AChE remained Endo H-sensitive (Fig. 3*A*, *lower panel*), *i.e.* never transit to the Golgi apparatus.

We also studied the effect of de-glycosylation on active/mature wild-type AChE by Endo H or PNGase F digestion. After the de-glycosylation by PNGase F, the enzymatic activity of AChE, expressed with or without PRiMA, was reduced by ~30% (Fig. 3*B*). In contrast, Endo H showed no effect on the enzymatic activity. The digestion of Endo H on the native enzyme showed a dose- and time-dependent manner, as revealed here by the protein pattern under a complete digestion of Endo H (supplemental Fig. 3). We also found that the elimination of glycans did not change the sedimentation properties or proportions of AChE molecular forms (Fig. 3*C*). This indicates that once the AChE protein has been correctly folded, the glycans are not required to maintain its catalytically active conformation or its oligomeric structure.

Effects of N-Glycosylation on the Assembly of G_4 AChE—We analyzed the influence of glycosylation on the assembly of PRiMA-linked AChE tetramers. The sedimentation profiles of AChE activity were similar for the wild-type AChE$_T^{WT}$ and for the un-glycosylated mutant AChE$_T^{N296Q/N381Q/N495Q}$, except for the difference in the level of enzymatic activity when expressed alone or with PRiMA (Fig. 4*A*). Like AChE$_T^{WT}$, AChE$_T^{N296Q/N381Q/N495Q}$ produced only G_1 and G_2 forms when expressed alone, whereas the G_4 form was produced when AChE$_T^{N296Q/N381Q/N495Q}$ was co-expressed with PRiMA-HA (HA epitope-tagged). To confirm whether the G_4 form was PRiMA-linked or not, we performed an immunodepletion assay using anti-HA antibody. The G_4 form of AChE$_T^{N296Q/N381Q/N495Q}$ was depleted by anti-HA antibody by ~80%, indicating that the G_4 enzymes, formed by AChE$_T^{WT}$ and AChE$_T^{N296Q/N381Q/N495Q}$, were associated with PRiMA (Fig. 4*A*).

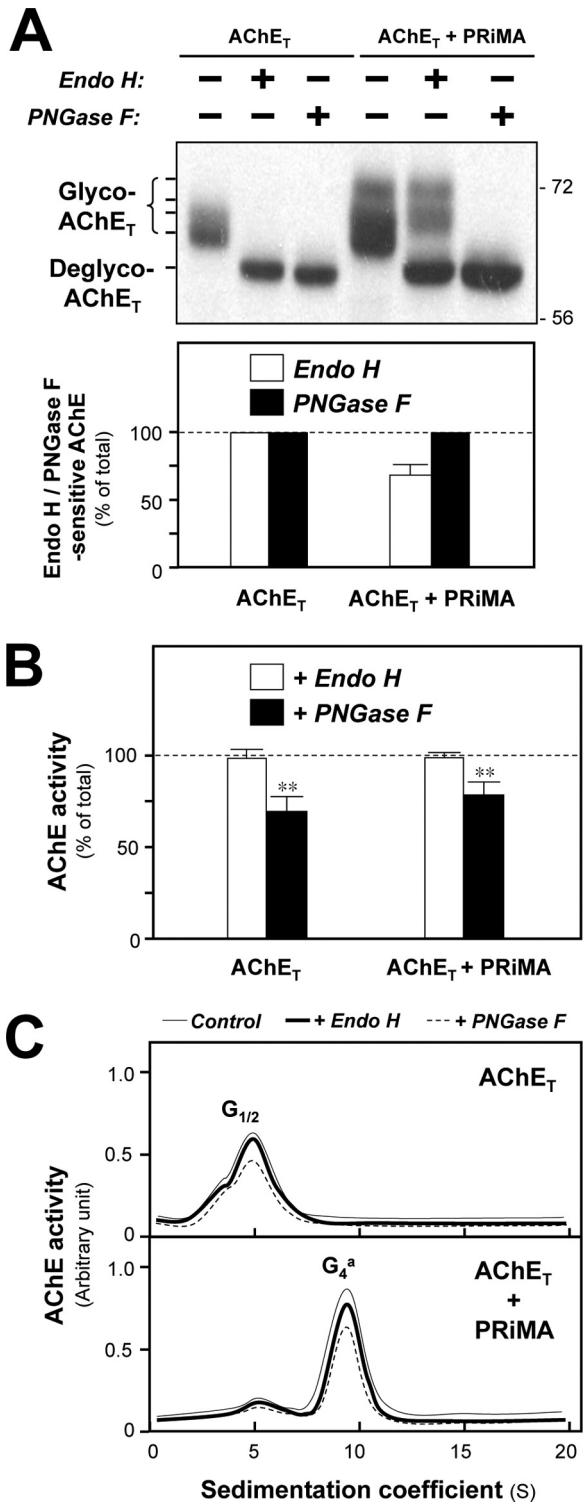

FIGURE 3. ***N*-Glycosylation is not required the catalytic activity of folded AChE$_T$ protein.** *A*, HEK293T cells were transfected with cDNAs encoding AChE$_T$ with or without cDNA encoding PRiMA. Equal amounts of protein from the cell lysates were incubated with or without Endo H or PNGase F under the non-denaturing conditions. The cell lysates were analyzed by SDS-PAGE and Western blotting with anti-AChE antibody (*upper panel*). The amount of the Endo H-sensitive or PNGase F-sensitive AChE$_T$ was quantified by calibrated densitometry (*lower panel*). The data are expressed as % of total AChE$_T$ protein. *B*, AChE enzymatic activity of the cell lysate from *A* was determined by Ellman assay. The data are expressed as % of total AChE activity before the treatment. *C*, the cell lysates from *A* were subjected to sucrose density gradient analysis. The enzymatic activities are plotted as a function of the S value, estimated from the position of the sedimentation markers. The enzymatic activities are expressed in arbitrary units. Representative gradient profiles and gels from four independent experiments are shown. Values are the means ± S.E. obtained in four independent experiments ($n = 4$). **, $p < 0.01$ compared with undigested control.

In addition, we determined the level of AChE$_T$ protein expression in different forms of AChE by quantification of Western blotting (Fig. 4*B*). Lysates from cells co-expressing AChE$_T^{WT}$ and PRiMA-HA or co-expressing AChE$_T^{N296Q/N381Q/N495Q}$ and PRiMA-HA, containing equal amounts of total protein, were subjected to sucrose-density gradient centrifugation. The enzymatic activity and AChE$_T^{WT}$ protein were determined in each fraction. The amount of AChE$_T$ protein correlated well with the enzymatic activity in the sucrose-density gradient (Fig. 4*B*), *i.e.* G_4 enzyme activity matched with the amount of AChE$_T$. On the other hand, the un-glycosylated G_4 enzyme, formed by AChE$_T^{N296Q/N381Q/N495Q}$ and PRiMA, shared similarity to that of the wild type. This confirmed that the un-glycosylated AChE$_T^{N296Q/N381Q/N495Q}$ mutant, like AChE$_T^{WT}$, was able to assemble with PRiMA to form an ~10 S sedimentating G_4 form, showing that *N*-glycosylation was not necessary for the oligomerization.

The subunit composition of the G_2 and G_4 forms was studied by non-denaturing gel electrophoresis. The G_2-enriched fractions, collected from cells expressing AChE$_T^{WT}$ in the absence of PRiMA, contained only monomers and dimers (Fig. 4*C*). Light dimers (no PRiMA), heavy dimers (with PRiMA), and tetramers (with PRiMA) were observed in the G_4-enriched fractions, as reported previously (21). We obtained identical results in the case of AChE$_T^{N296Q/N381Q/N495Q}$, which suggested the oligomerization of AChE dimer or tetramer was not affected by the glycosylation of AChE$_T$.

The influence of *N*-glycosylation on the thermal stability of different forms of AChE$_T^{WT}$ and AChE$_T^{N296Q/N381Q/N495Q}$ was determined by comparing the time-dependent loss of enzymatic activity at different temperatures. The $G_{1/2}$ fractions were obtained from cells expressing AChE$_T^{WT}$ or AChE$_T^{N296Q/N381Q/N495Q}$ without PRiMA, and the G_4 fractions were obtained from cells expressing AChE$_T^{WT}$ or AChE$_T^{N296Q/N381Q/N495Q}$ with PRiMA. At 4 °C, $G_{1/2}$ and G_4 forms of AChE$_T^{WT}$ or AChE$_T^{N296Q/N381Q/N495Q}$ were rather stable, *i.e.* the enzymatic activity did not change over a period of 1 h (Fig. 5). At 25 and 45 °C, AChE$_T^{N296Q/N381Q/N495Q}$ presented a significant decrease in the enzymatic activity (Fig. 5). The rank order of thermal sensitivity was G_4 AChE$_T^{WT}$ > $G_{1/2}$ AChE$_T^{WT}$ > G_4 AChE$_T^{N296Q/N381Q/N495Q}$ > $G_{1/2}$ AChE$_T^{N296Q/N381Q/N495Q}$. This indicates that the *N*-glycans of AChE contribute to the enzyme stability.

Effects of N-Glycosylation on the Trafficking of PRiMA-linked G_4 AChE—Although the abolishment of *N*-glycosylation on AChE$_T$ subunits did not prevent their assembly with PRiMA, it might affect the proper trafficking of the oligomeric protein. To address this question, subcellular fractionation was performed to determine the distribution of AChE$_T$ in cultures expressing AChE$_T^{WT}$ or AChE$_T^{N296Q/N381Q/N495Q}$ together with PRiMA-HA. The subcellular compartments were separated in continuous iodixanol gradients and identified by Western blotting with specific antibodies against different marker proteins. The PM

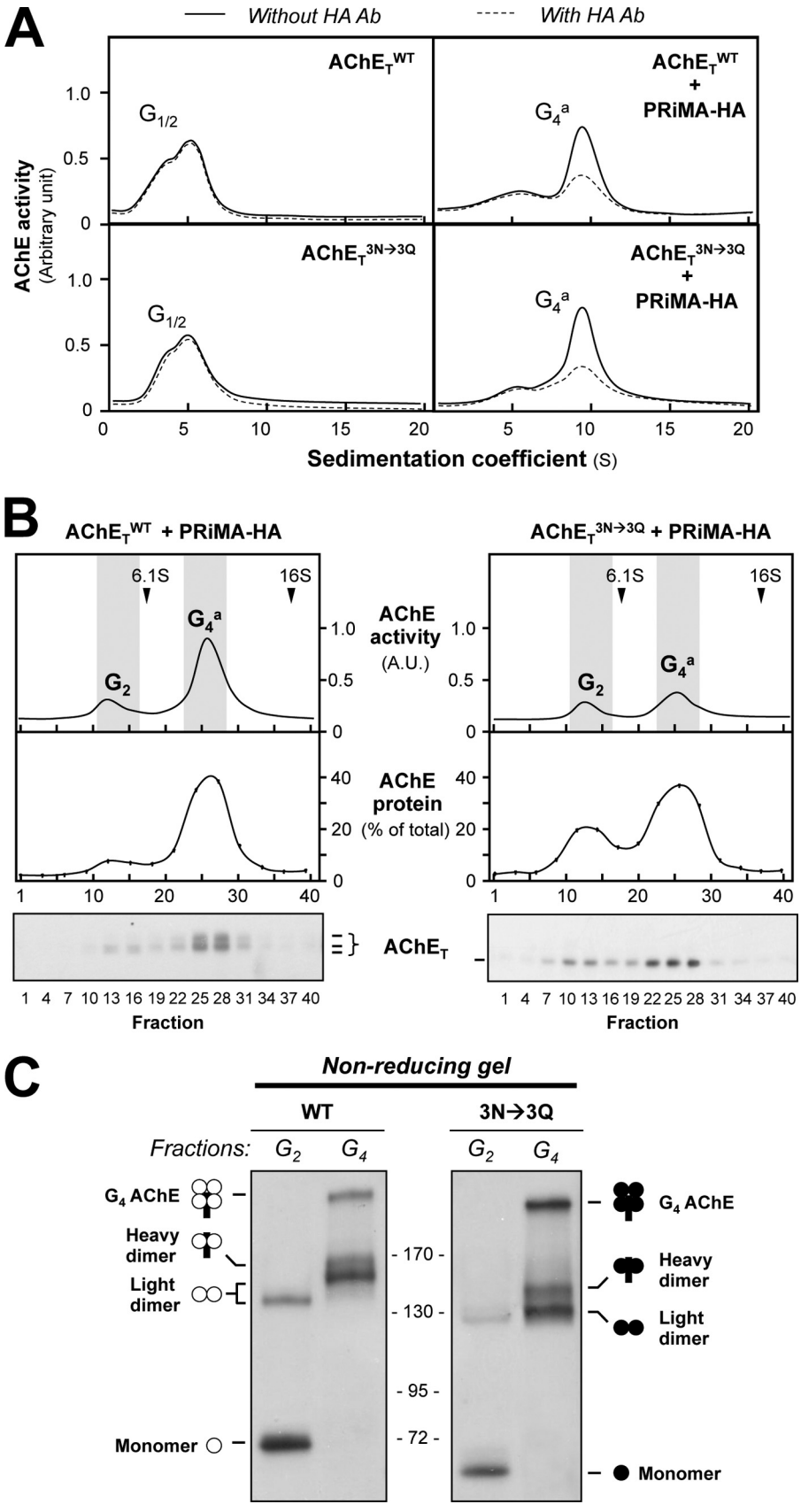
A
Without HA Ab
With HA Ab
AChE$_T^{WT}$
AChE$_T^{WT}$ + PRiMA-HA
AChE$_T^{3N→3Q}$
AChE$_T^{3N→3Q}$ + PRiMA-HA
G$_{1/2}$
G$_4^a$
AChE activity (Arbitrary unit)
Sedimentation coefficient (S)
B
AChE$_T^{WT}$ + PRiMA-HA
AChE$_T^{3N→3Q}$ + PRiMA-HA
6.1S
16S
G$_2$
G$_4^a$
AChE activity (A.U.)
AChE protein (% of total)
AChE$_T$
Fraction
C
Non-reducing gel
WT
3N→3Q
Fractions: G$_2$ G$_4$
G$_4$ AChE
Heavy dimer
Light dimer
Monomer
- 170 -
- 130 -
- 95 -
- 72 -

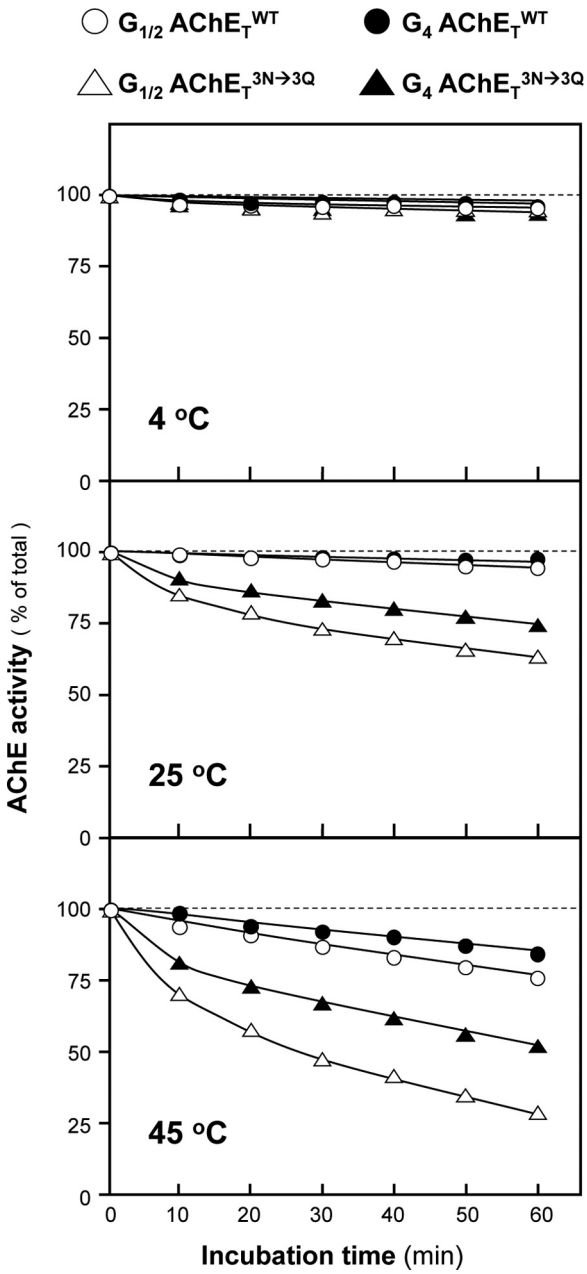

FIGURE 5. **The thermostability of glycan-depleted PRiMA-linked G_4 AChE.** $G_{1/2}$ and G_4 fractions of $AChE_T^{WT}$ or $AChE_T^{N296Q/N381Q/N495Q}$ from Fig. 4 were incubated at 4, 25, and 55 °C. Samples were collected at 10-min intervals from 0 to 60 min and chilled on ice, and their residual enzymatic activity was determined. The data are expressed as the % of the original activity (time 0). Values are the means ± S.E., with triplicate samples ($n = 3$). The S.E. *bars* are not shown for clarity (<5% of the means).

marker (Na^+/K^+-ATP) and the Golgi marker (GM130) were found at the top of the gradient, *i.e.* fractions 2–4, whereas the ER marker (calnexin) was enriched at the bottom of the gradient, *i.e.* fractions 8–10 (Fig. 6*A*). The last fraction was excluded because of the contamination of aggregated proteins. In cells co-expressing $AChE_T^{WT}$ and PRiMA-HA, $AChE_T$ underwent a typical pattern of ER-to-Golgi maturation, with the majority of mature $AChE_T$ (heavily glycosylated) localized in Golgi/PM fractions (Fig. 6*A*). In contrast, the glycosylation mutant $AChE_T^{N296Q/N381Q/N495Q}$ was localized almost exclusively in the ER fractions, with only a very small proportion in the Golgi/PM fractions (Fig. 6*A*). Similarly, the other glycosylation mutants were predominantly localized in ER fractions; but the extent was not as severe as that of $AChE_T^{N296Q/N381Q/N495Q}$ mutant (supplemental Fig. 4*A*). Fig. 6*B* shows the quantitative distribution of $AChE_T$ in different subcellular organelles. In the absence of glycosylation, $AChE_T^{N296Q/N381Q/N495Q}$ protein was retained in the ER and failed to be transported to the Golgi apparatus. In $AChE_T^{WT}$ expression, the enzymatic activity was in line to the protein expression, *i.e.* higher activity in the Golgi apparatus. In contrast, the ER-retained $AChE_T^{N296Q/N381Q/N495Q}$, although in high abundance, showed very little enzymatic activity (Fig. 6*B*). These phenomena were also applied to other mutants (supplemental Fig. 4*B*). This result was in line with the low enzymatic activity of the un-glycosylated $AChE_T^{N296Q/N381Q/N495Q}$ mutant. In addition, all $AChE_T$, within the G_4 enzyme formed by $AChE_T$ and PRiMA, in the ER was sensitive to Endo H or PNGase F digestion, whereas only ~30% in Golgi/PM fraction was Endo H-sensitive (Fig. 6*C*).

Because $AChE_T^{N296Q/N381Q/N495Q}$ is able to assemble with PRiMA to form a PRiMA-linked G_4 enzyme, it is interesting to know whether the ER-retained fraction is PRiMA-linked or not. We, therefore, examined whether G_4 AChE from each fraction was associated with the PRiMA-HA construct, identified with an anti-HA antibody (Fig. 6*D*). The molecular forms of AChE were analyzed by sucrose-density gradient. In both cases of enzymes formed by $AChE_T^{WT}$ and $AChE_T^{N296Q/N381Q/N495Q}$ with PRiMA, we found that the ER-enriched fractions contained a G_4 form that could be immuno-depleted by the anti-HA antibody (Fig. 6*D*), indicating that it was PRiMA-linked. In contrast to $AChE_T^{WT}$, the glycan-depleted AChE (formed by $AChE_T^{N296Q/N381Q/N495Q}$) was not recovered in the Golgi/PM-enriched fractions (Fig. 6*D*). Thus, in the absence of *N*-glycosylation, $AChE_T$ could assemble with PRiMA to form a PRiMA-linked G_4 enzyme, but the oligomer failed to be exported from the ER to the Golgi apparatus.

The trafficking of AChE was further analyzed by immunofluorescence staining of transfected cells that expressed $AChE_T^{WT}$ or $AChE_T^{N296Q/N381Q/N495Q}$ together with PRiMA. The cells were stained with the anti-AChE antibody with or without permeabilization by Triton X-100. An intense immunoreactivity was observed for both $AChE_T^{WT}$

FIGURE 4. ***N*-Glycosylation of $AChE_T$ is not required for its assembly with PRiMA.** *A*, HEK293T cells were transfected with the cDNAs encoding $AChE_T^{WT}$ or $AChE_T^{N296Q/N381Q/N495Q}$ with or without PRiMA-HA. Cell lysates containing equal amounts of AChE activity were incubated with or without an anti-HA antibody (*Ab*). After precipitation by protein G-agarose, the supernatants were subjected to sucrose density gradient analysis. *B*, cell lysates containing equal amounts of total protein were subjected to sucrose density gradient analysis. Fractions were assayed for AChE enzymatic activity and $AChE_T$ protein by Western blotting. The *upper panel* shows the enzymatic activity, whereas the *middle* and *lower panels* indicate the amount of $AChE_T$ protein in selected fractions. Sedimentation markers are shown. The enzymatic activities are expressed in arbitrary units (*A.U.*), and the protein is shown as % of total $AChE_T$ protein. *C*, G_2 and G_4 fractions, corresponding to the shaded zones of the gradients in *B*, were analyzed by non-reducing electrophoresis and Western blotting with the anti-AChE antibody. Representative gradient profiles and gels from three independent experiments are shown ($n = 3$).

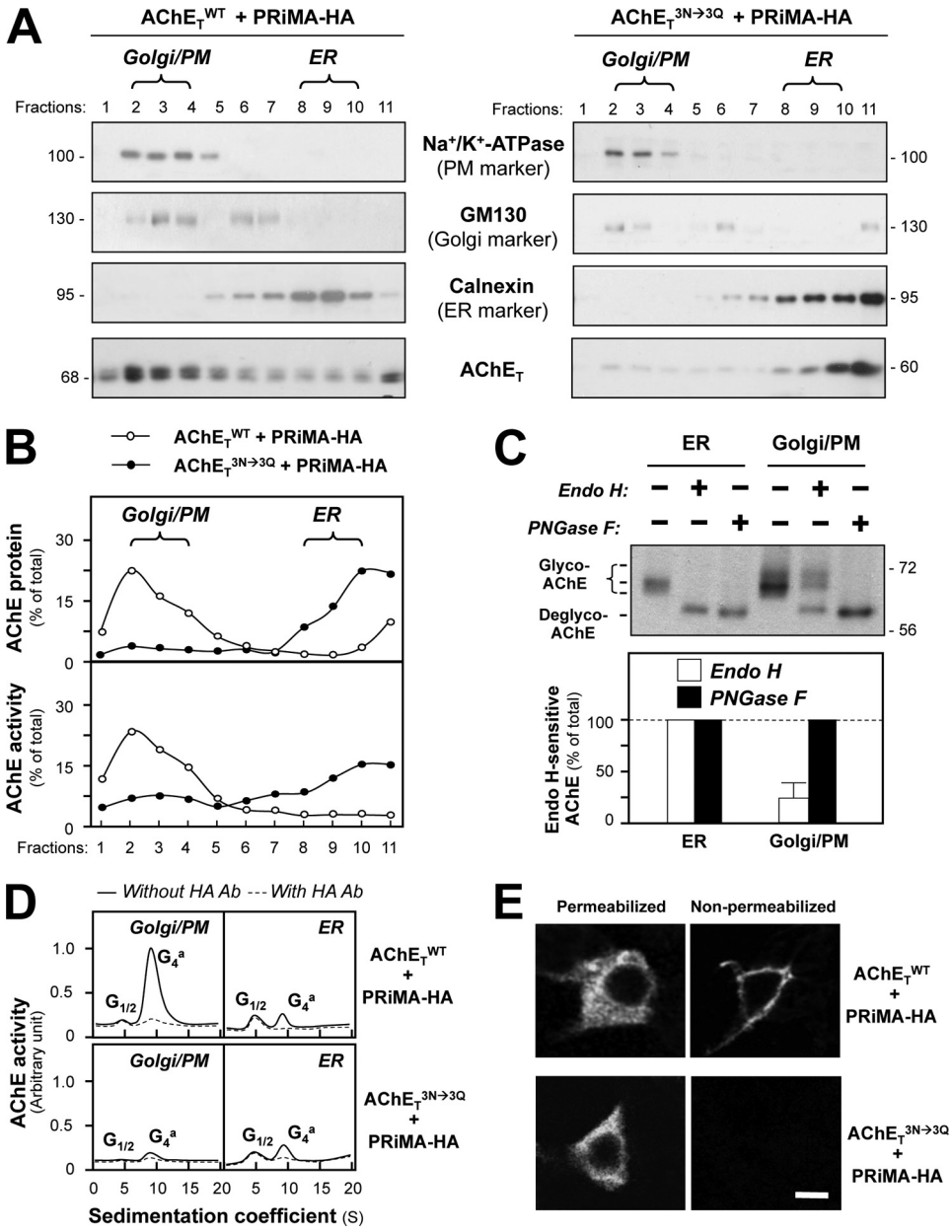

FIGURE 6. ***N*-Glycosylation is necessary for the trafficking of PRiMA-linked G_4 AChE.** *A*, HEK293T cells were transfected with the cDNAs encoding $AChE_T^{WT}$ or $AChE_T^{N296Q/N381Q/N495Q}$ and PRiMA-HA. After 48 h the transfected cells were subjected to subcellular fractionation using a continuous iodixanol density gradient, and 11 fractions were collected. The distribution of ER (fractions 8–10) and Golgi/PM (plasma membrane) (fractions 2–4) subcellular compartments was determined by immunoblotting samples from each fraction with marker proteins, Na^+/K^+-ATP (PM), GM130 (Golgi) and calnexin (ER). The distribution of $AChE_T$ protein was analyzed by immunoblotting with the anti-AChE antibody. *B*, the amount of $AChE_T$ protein or AChE activity in each fraction was quantified from the blots (*A*) by calibrated densitometry. The data are expressed as the % of total $AChE_T$ protein (*upper panel*) or AChE activity (*lower panel*). *C*, samples of ER- and Golgi/PM-enriched fractions from cells co-expressing $AChE_T^{WT}$ and PRiMA-HA were incubated with Endo H or PNGase F (*upper panel*). The proportion of Endo H-sensitive or PNGase F-sensitive $AChE_T$ was quantified by calibrated densitometry (*lower panel*). The data are expressed as % of the total $AChE_T$ protein. *D*, samples from ER- and Golgi/PM-enriched fractions from *A* were incubated with and without anti-HA antibody (*Ab*, 1:1000, Sigma). After precipitation by protein G-agarose, the supernatants were subjected to sucrose density gradient analysis. The enzymatic activities are plotted as a function of the S value, estimated from the position of the sedimentation markers. The enzymatic activities are expressed in arbitrary units. *E*, transfected HEK293T cells as in *A* were immuno-stained with the anti-AChE antibody without permeabilization, showing AChE exposed at the plasma membrane and with permeabilization by Triton X-100 (0.2%) showing AChE in subcellular compartments. *Bar*, 20 μm.

and $AChE_T^{N296Q/N381Q/N495Q}$ in permeabilized cells, indicating that both proteins were expressed at similar levels (Fig. 6*E*). Without permeabilization, the staining was detected on the plasma membrane of cells expressing $AChE_T^{WT}$ but not $AChE_T^{N296Q/N381Q/N495Q}$ (Fig. 6*E*). This supports our conclusion that *N*-glycans are required for the proper membrane targeting of PRiMA-linked G_4 AChE.

Formation of Interspecies Chicken-Human AChE G_4 Hybrids—We have shown that mammalian and chicken $AChE_T$ subunits can form mixed $AChE_T$ dimers or tetramers, in agreement with the notion that this association depends on the "four-helix-bundle" contact between two catalytic domains (21). To investigate whether glycosylated and un-glycosylated $AChE_T$ subunits possess the same capacity for dimeric

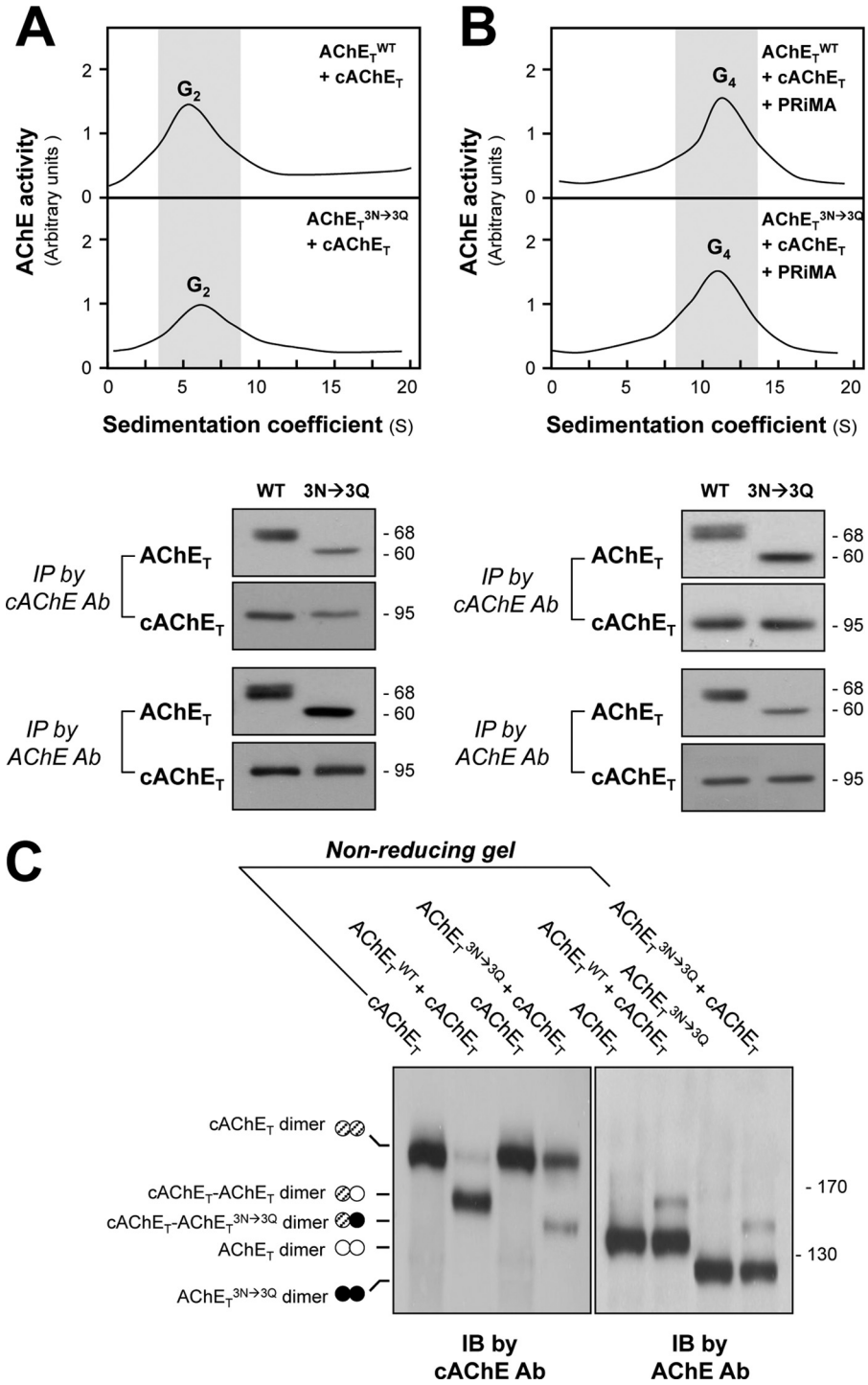

FIGURE 7. ***N*-Glycosylation is not required for the formation of human-chicken AChE dimers and tetramers.** *A*, HEK293T cells were transfected with equal amounts of cDNAs encoding human $AChE_T$ or $AChE_T^{N296Q/N381Q/N495Q}$ together with chicken $AChE_T$ (*$cAChE_T$*). Equal amounts of protein from cell lysates were subjected to sucrose density gradient analysis. The enzymatic activities are plotted as a function of the S value, estimated from the position of sedimentation markers (*upper panel*). G_2 fractions were collected for immunoprecipitation (*IP*) by either anti-human AChE antibody (*Ab*) or anti-cAChE antibody. The immunoprecipitated complexes were analyzed by SDS-PAGE and Western blotting with anti-AChE and anti-cAChE antibodies, as indicated (*lower panel*). Both antibodies did not cross-react with other corresponding antigen. *B*, HEK293T cells were transfected with equal amount of cDNAs encoding $AChE_T$ or $AChE_T^{N296Q/N381Q/N495Q}$ together with $cAChE_T$ and PRiMA. Equal amounts of protein from cell lysates were subjected to sucrose density gradient analysis as in *A*. G_4 fractions were collected for immunoprecipitation as in *A*. *C*, extracts from cells expressing $AChE_T^{WT}$ and $cAChE_T$ separately or together were analyzed by non-reducing SDS-PAGE and labeled with anti-cAChE and anti-AChE antibodies. The presence of an intermediate band between cAChE and $AChE_T^{N296Q/N381Q/N495Q}$ dimers, recognized by both antibodies, demonstrates the formation of mixed $cAChE_T$-$AChE_T^{N296Q/N381Q/N495Q}$ dimers. *IB*, immunoblot.

assembly, we co-expressed human $AChE_T^{WT}$ or its glycosylation mutant $AChE_T^{N296Q/N381Q/N495Q}$ with chicken $AChE_T$ ($cAChE_T$) in HEK293T cells in the presence or absence of PRiMA. When expressed without PRiMA, the co-expression of $AChE_T^{WT}$ and $cAChE_T$ or of $AChE_T^{N296Q/N381Q/N495Q}$ and $cAChE_T$ produced mainly G_2 dimers (Fig. 7*A*, *upper panel*).

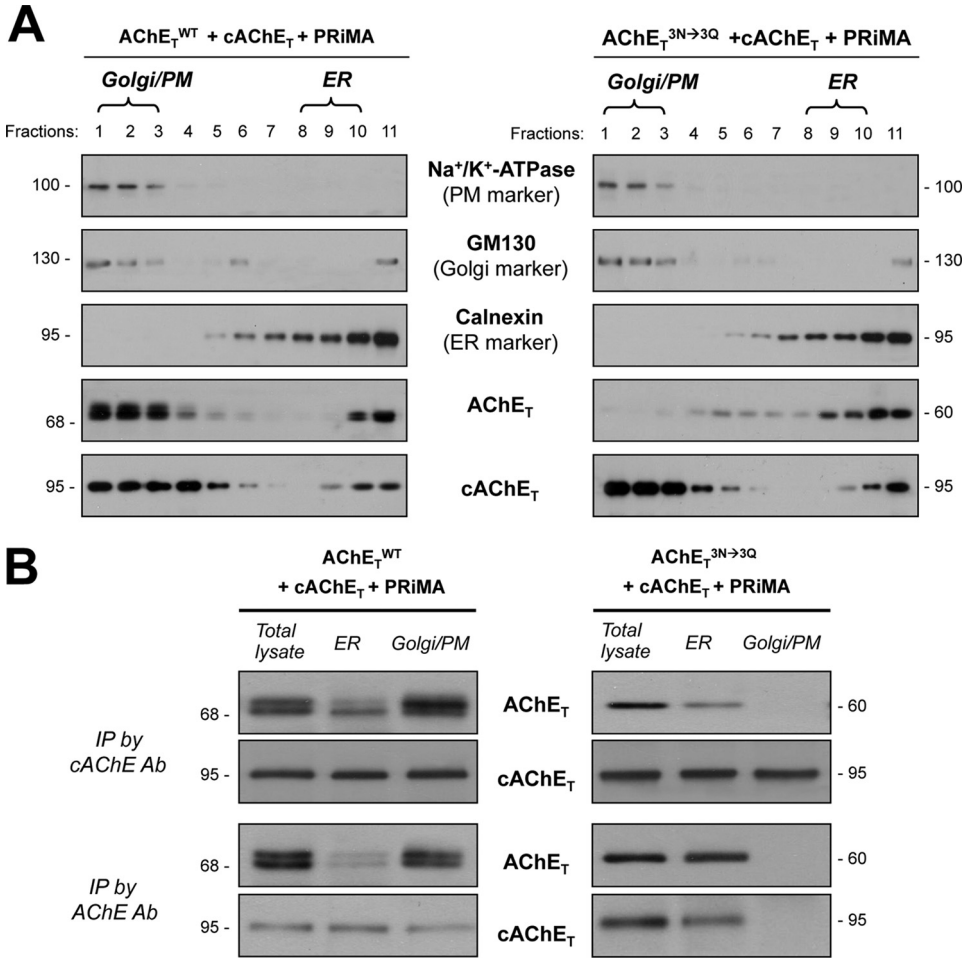

FIGURE 8. ***N*-Glycosylation is required for the trafficking of PRiMA-linked mixed chicken-human AChE tetramer.** *A*, HEK293T cells were transfected with the cDNAs encoding AChE$_T^{WT}$ or AChE$_T^{N296Q/N381Q/N495Q}$ together with cAChE$_T$ and PRiMA. After 48 h the transfected cells were subjected to subcellular fractionation, and the distribution of ER and Golgi/PM subcellular compartments was determined by immunoblotting as in Fig. 6*A*. The distribution of AChE$_T$ and cAChE$_T$ proteins was analyzed by immunoblotting with the anti-AChE antibodies. *B*, protein extracts from the total lysate and ER-enriched and Golgi/PM-enriched fractions of the transfected cells from *A* were immunoprecipitated (*IP*) by either anti-human AChE antibody or anti-chicken AChE antibody (*Ab*). The immunoprecipitated complexes were analyzed by SDS-PAGE and Western blotting with anti-human AChE and anti-chicken AChE antibodies as indicated. Representative gels from three independent experiments are shown.

The formation of mixed, interspecies dimers was examined by immunoprecipitation with anti-human and anti-chicken AChE antibodies using the G_2-enriched fractions obtained from sucrose density gradients (Fig. 7*A*, *lower panel*). As previously reported (21), AChE$_T^{WT}$ could be pulled down by the anti-chicken AChE antibody, and this was also the case for AChE$_T^{N296Q/N381Q/N495Q}$, showing that it can also associate with cAChE$_T$ in mixed human-chicken dimers. AChE$_T^{WT}$ and cAChE$_T$ as well as AChE$_T^{N296Q/N381Q/N495Q}$ and cAChE$_T$ were also co-expressed with PRiMA in HEK293T cells, producing G_4 forms of AChE (Fig. 7*B*, *upper panel*). Immunoprecipitation experiments confirmed that cAChE$_T$ could associate with AChE$_T^{WT}$ or AChE$_T^{N296Q/N381Q/N495Q}$ in mixed PRiMA-linked tetramers (Fig. 7*B*, *lower panel*). Therefore, PRiMA is able to recruit human and chicken AChE$_T$ subunits into mixed tetramers, even for the un-glycosylated AChE$_T^{N296Q/N381Q/N495Q}$ subunits.

The formation of a dimer involves a disulfide linkage near the C terminus of the two AChE$_T$ subunits (21). To further confirm the formation of interspecies dimers between AChE$_T^{N296Q/N381Q/N495Q}$ and cAChE$_T$, we performed non-reducing gel electrophoresis and Western blotting (Fig. 7*C*). In lysates from cells co-expressing AChE$_T^{WT}$ and cAChE$_T$, we observed the presence of cAChE$_T$ dimers (~190 kDa), AChE$_T^{WT}$ dimers (~140 kDa), and an intermediate heterodimer (~165 kDa; AChE$_T^{WT}$-cAChE$_T$ dimer) that was labeled by both anti-chicken and anti-human AChE antibodies. Similarly, co-expression of AChE$_T^{N296Q/N381Q/N495Q}$ and cAChE$_T$ produced cAChE$_T$ dimers, AChE$_T^{N296Q/N381Q/N495Q}$ dimers (~125 kDa) and an intermediate heterodimer (~155 kDa) that could also be labeled by both antibodies. Moreover, the proportion of the heterodimer formed was normally lower that that of the total cAChE$_T$ dimer and total human AChE$_T$ dimer (Fig. 7*C*). This might be caused by the various stabilities of different dimers or the preference of the subunit selection during the dimer formation. Thus, the glycosylated and un-glycosylated AChE$_T$ could form interspecies dimers, indicating that the contact between two subunits in a dimer does not depend on the glycosylation.

We further analyzed the traffic of mixed PRiMA-linked AChE$_T^{N296Q/N381Q/N495Q}$-cAChE$_T$ tetramers. Does the glycosylated cAChE$_T$ rescue AChE$_T^{N296Q/N381Q/N495Q}$ from being

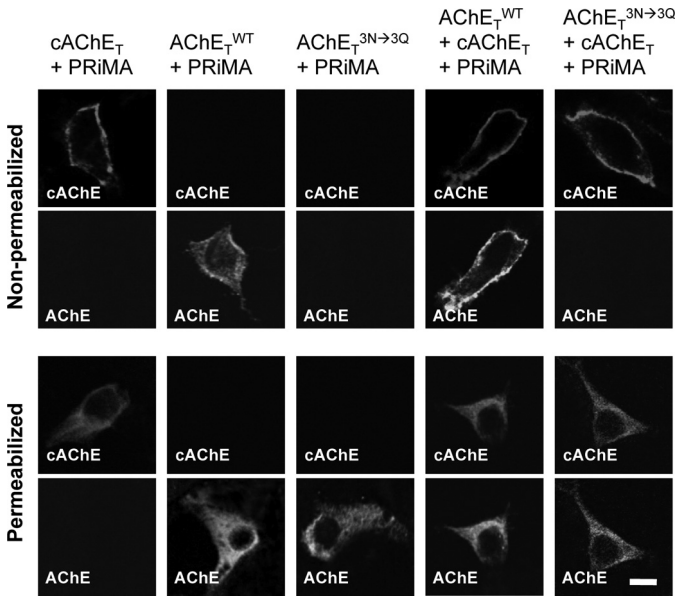

FIGURE 9. ***N*-Glycosylation is required for the plasma membrane targeting of PRiMA-linked mixed chicken-human AChE tetramer.** HEK293T cells were transfected with different combinations of cDNAs as indicated. After 48 h, cells were immuno-stained with anti-chicken AChE or anti-human AChE antibody without or with permeabilization by Triton X-100 (0.2%) to visualize AChE on the plasma membrane or total AChE, including subcellular compartments, respectively. *Bar*, 20 μm.

retained in the ER? In cultured cells expressing AChE$_T^{WT}$ or AChE$_T^{N296Q/N381Q/N495Q}$ with cAChE$_T$ and PRiMA (as in Fig. 7), the subcellular fractionation was performed to determine the distribution of AChE$_T$ in the cultures. As expected, the mixed PRiMA-linked tetramer, formed by AChE$_T^{WT}$ and cAChE$_T$, underwent a typical pattern of ER-to-Golgi maturation, with the majority of mature AChE$_T$ (heavy glycosylated) localized in Golgi/PM fractions (Fig. 8*A*, *left panel*). In contrast, the mixed PRiMA-linked tetramer formed by AChE$_T^{N296Q/N381Q/N495Q}$ and cAChE$_T$ was extensively localized in the ER fractions (Fig. 8*A*, *right panel*), *i.e.* high level of AChE$_T^{N296Q/N381Q/N495Q}$ being retained in the ER. The cAChE$_T$ was still predominantly localized in the Golgi/PM fractions; because of the formation of intraspecies chicken G$_4$ AChE, *i.e.* PRiMA-linked cAChE$_T$. The proper formation of interspecies of G$_4$ AChE was confirmed by the immunoprecipitation in the cell lysates received from different subcellular compartments. As expected, the mixed PRiMA-linked tetramer, formed by AChE$_T^{WT}$ and cAChE$_T$, was precipitated by either anti-human (recognized at ~68 kDa bands) or anti-chicken AChE (recognized at ~95 kDa bands) antibodies (Fig. 8*B*); this mixed enzyme was revealed in both ER and Golgi/PM fractions. In contrast, the G$_4$ AChE$_T^{N296Q/N381Q/N495Q}$-cAChE$_T$ enzyme was only revealed in the ER fractions, which was absent in the Golgi/PM fractions (Fig. 8*B*). Thus, the rescue of AChE$_T^{N296Q/N381Q/N495Q}$-cAChE$_T$ mixed tetramer being retained in the ER by the glycosylated cAChE$_T$ was not possible.

In addition, we immuno-stained surface proteins in transfected HEK293T, expressing PRiMA-linked AChE$_T$-cAChE$_T$ mixed tetramers (see also Fig. 7). Both AChE$_T^{WT}$ and cAChE$_T$ could be detected on the surface of cells co-expressing these two subunits with PRiMA (Fig. 9). In contrast, we observed no human AChE on the surface of cells co-expressing the un-glycosylated AChE$_T^{N296Q/N381Q/N495Q}$ mutant together with cAChE and PRiMA, indicating that the PRiMA-linked cAChE$_T$-AChE$_T^{N296Q/N381Q/N495Q}$ and AChE$_T^{N296Q/N381Q/N495Q}$-AChE$_T^{N296Q/N381Q/N495Q}$ tetramers did not reach the plasma membrane but probably remained trapped in the ER. Therefore, the un-glycosylation on one of the AChE$_T$ subunits in the tetramer appears to represent efficient the ER retention signals.

DISCUSSION

In the present study, we analyzed the effects of *N*-glycosylation on the enzymatic activity and oligomerization of PRiMA-linked G$_4$ AChE. The enzymatic activity was significantly affected by glycosylation, but this post-translational modification showed no effect on the assembly of PRiMA-linked G$_4$ AChE. The enzymatic activities of G$_4$ AChE, formed by AChE$_T^{N296Q}$ and AChE$_T^{N495Q}$, were reduced to 70~80% of AChE$_T^{WT}$, whereas the enzymatic activity of G$_4$ AChE$_T^{N381Q}$ was dramatically reduced to ~10% only. The glycan-depleted tetrameric AChE (AChE$_T^{N296Q/N381Q/N495Q}$) possessed less than 5% of the enzymatic activity of wild type. This indicates that the oligosaccharides, carried by the three glycosylation sites, function in a co-operative manner. Kinetic analyses further confirmed an increase of K_m values in glycan-depleted AChEs as compared with the wild-type enzyme. On the other hand, the removal of oligosaccharide side chains from mature AChE molecules by Endo H/PNGase F did not seem to alter the overall structure of the protein because most of the AChE activity was retained after the de-glycosylation. Therefore, the *N*-glycosylation plays an important role in assisting the folding of newly synthesized AChE$_T$ protein, but the conformation of catalytically active (fully folded) G$_4$ AChE no longer depends on the presence of *N*-linked carbohydrates.

The glycosylation of AChE$_T$ did not appear to play a significant role in oligomerization of PRiMA-linked G$_4$ AChE. The glycan-depleted AChE$_T^{N296Q/N381Q/N495Q}$ mutant could form oligomers, which appeared structurally similar to that of the wild-type enzyme, including (i) identical sedimentation in sucrose density gradients, (ii) identical organization of disulfide linkages in dimers and in PRiMA-linked tetramers, and (iii) identical ability to form interspecies dimers and/or tetramers. Structural studies have shown that the dimerization of AChE$_T$ depends on the formation of a four-helix-bundle, in which two α-helices of each catalytic domain are closely apposed with the corresponding helices of the other one (30, 31). Indeed, the four-helix-bundle is highly conserved among different species of AChE catalytic subunits (21). On the other hand, the formation of AChE tetramer depends on the presence of a C-terminal t-peptide (21, 31, 32) of AChE$_T$. The assembly of a tetramer is efficiently induced by a proline-rich attachment domain-containing protein, ColQ or PRiMA (8, 33), that interacts with the AChE$_T$ t-peptide. Thus, the proper folding of a catalytically active AChE monomer and the assembly of AChE$_T$ subunits into a PRiMA-linked tetramer are two independent events.

ER is the entry point into the "classical" secretory pathway for most membrane-bound and secreted proteins (34) and exerts an efficient "quality control" that ensures that proteins are cor-

rectly folded before allowing their transit to the Golgi apparatus and beyond. It is generally believed that *N*-linked glycosylation participates in the control of protein folding and intracellular trafficking and that this post-translational modification also protects proteins from proteolytic degradation (14, 35). Consistent with our current understanding of glycoprotein metabolism, the synthesis and processing of PRiMA-linked G_4 $AChE_T$ follows an orderly sequence of events beginning with the sequestering of the nascent polypeptide chain and the addition of preassembled oligosaccharides in the ER followed by transfer into the Golgi apparatus and modification of the glycan chains. When the sites of *N*-glycosylation are eliminated, the folding of $AChE_T$ partially fails, leading to a severe loss of the enzymatic activity. Although the glycan-depleted $AChE_T$ can still assemble with PRiMA to form PRiMA-linked G_4 AChE in the ER, the oligomeric enzyme failed to be exported to the Golgi apparatus. Our results show that the assembly of PRiMA-linked G_4 AChE is completed in the ER, not in the Golgi, and that the suppression of *N*-glycosylation can prevent the trafficking of assembled AChE. The ultimate fate of glycan-depleted and less active AChE is probably degradation, *e.g.* via quality control chaperons, *e.g.* calnexin/calreticulin that targets the misfolded proteins for degradation and prevents them proceeding from ER to Golgi. The control of glycosylation, therefore, could be as a means in regulating the level of functional AChE in the brain. Supporting this notion, the alteration in AChE glycosylation has been reported in the brain and cerebrospinal fluid of patients from Alzheimer disease (17).

The biogenesis of ColQ-associated AChE in muscle has been extensively studied by Rotundo and co-workers (36–38). Their results suggest that (i) the assembly of dimers and/or tetramers occurs in the ER, and the association with ColQ is completed in the Golgi apparatus; (ii) about 70–80% of the total newly synthesized Endo H-sensitive AChE enzyme does not transit to Golgi apparatus and undergoes a rapid degradation; (iii) a small fraction of AChE is processed in Golgi apparatus, where it becomes Endo H-insensitive and is exported. By using recombinant DNA in an expression system, our current results accord with the studies by Rotundo and co-workers (36–38). First, the assembly of PRiMA-linked G_4 AChE having minimal glycosylation is completed in the ER; the ER-retained enzymes are mainly Endo H-sensitive. Second, the full glycosylated $AChE_T$ should have a transit to Golgi apparatus and acquire further glycosylation that is Endo H-insensitive. This fully glycosylated enzyme reaches the plasma membrane as a functional enzyme. Third, the glycan-depleted AChE, as generated here by the mutants, could represent the partial glycosylated AChE, *i.e.* they are retained in ER, enzymatic less active and unstable. Contrarily, the ColQ-linked AChE (A_{12} form) was proposed to be fully assembled in the Golgi apparatus (16) instead of being assembled in the ER, as revealed here for the PRiMA-linked tetramers. On top of the aforementioned evidences, we would like to propose that the glycan-depleted AChE corresponds to the fraction of enzymatically less active AChE that is retained and degraded in the ER, as described in avian tissues (36, 39). In line with this notion, the specific activity of AChE, normalized to AChE protein, is lower in the ER than that in the Golgi apparatus. Thus the transit from the ER to the Golgi apparatus would depend on the completion or not of *N*-glycosylation of $AChE_T$. Moreover, a glycan-depleted PRiMA-linked AChE was shown here to be enzymatically less active. However, the inactive or less active AChE reported previously in chicken brain (39) or in muscle (36, 40, 41) was restricted to the G_1 and G_2 forms, not the G_4 form. A possible explanation for this discrepancy could be the partially glycosylated and poorly active G_4 AChE is processed to degradation rapidly *in vivo*.

Acknowledgments—We thank Prof. Avigdor Shafferman from the Department of Biochemistry and Molecular Genetics, Israel Institute for Biological Research, Ness-Ziona, Israel for the cDNAs encoding the un-glycosylated mutants of human $AChE_T$. In addition we are grateful to Drs. Jean Massoulié and Suzanne Bon from the Institut de Biologie de l'Ecole Normale Supérieure, Paris, France, for advice during the study.

REFERENCES

1. Massoulié, J., Pezzementi, L., Bon, S., Krejci, E., and Vallette, F. M. (1993) *Prog. Neurobiol.* **41,** 31–91
2. Krejci, E., Thomine, S., Boschetti, N., Legay, C., Sketelj, J., and Massoulié, J. (1997) *J. Biol. Chem.* **272,** 22840–22847
3. Massoulié, J., and Millard, C. B. (2009) *Curr. Opin. Pharmacol.* **9,** 316–325
4. Perrier, A. L., Massoulié, J., and Krejci, E. (2002) *Neuron* **33,** 275–285
5. Mok, M. K., Leung, K. W., Xie, H. Q., Guo, A. J., Chen, V. P., Zhu, J. T., Choi, R. C., and Tsim, K. W. (2009) *Neurosci. Lett.* **461,** 202–206
6. Xie, H. Q., Liang, D., Leung, K. W., Chen, V. P., Zhu, K. Y., Chan, W. K., Choi, R. C., Massoulié, J., and Tsim, K. W. (2010) *J. Biol. Chem.* **285,** 11537–11546
7. Xie, H. Q., Choi, R. C., Leung, K. W., Siow, N. L., Kong, L. W., Lau, F. T., Peng, H. B., and Tsim, K. W. (2007) *J. Biol. Chem.* **282,** 11765–11775
8. Bon, S., Coussen, F., and Massoulié, J. (1997) *J. Biol. Chem.* **272,** 3016–3021
9. Dvir, H., Harel, M., Bon, S., Liu, W. Q., Vidal, M., Garbay, C., Sussman, J. L., Massoulié, J., and Silman, I. (2004) *EMBO J.* **23,** 4394–4405
10. Liao, J., Heider, H., Sun, M. C., and Brodbeck, U. (1992) *J. Neurochem.* **58,** 1230–1238
11. Liao, J., Heider, H., Sun, M. C., Stieger, S., and Brodbeck, U. (1991) *Eur. J. Biochem.* **198,** 59–65
12. Tsim, K. W., Randall, W. R., and Barnard, E. A. (1988) *J. Neurochem.* **51,** 95–104
13. Méflah, K., Bernard, S., and Massoulié, J. (1984) *Biochimie* **66,** 59–69
14. Helenius, A. (1994) *Mol. Biol. Cell* **5,** 253–265
15. Velan, B., Kronman, C., Ordentlich, A., Flashner, Y., Leitner, M., Cohen, S., and Shafferman, A. (1993) *Biochem. J.* **296,** 649–656
16. Rotundo, R. L. (1984) *Proc. Natl. Acad. Sci. U.S.A.* **81,** 479–483
17. Sáez-Valero, J., Barquero, M. S., Marcos, A., McLean, C. A., and Small, D. H. (2000) *J. Neurol. Neurosurg. Psychiatry* **69,** 664–667
18. Mimori, Y., Nakamura, S., and Yukawa, M. (1997) *Behav. Brain Res.* **83,** 25–30
19. Noureddine, H., Carvalho, S., Schmitt, C., Massoulié, J., and Bon, S. (2008) *J. Biol. Chem.* **283,** 20722–20732
20. Gough, N. R., and Randall, W. R. (1995) *J. Neurochem.* **65,** 2734–2741
21. Chen, V. P., Xie, H. Q., Chan, W. K., Leung, K. W., Chan, G. K., Choi, R. C., Bon, S., Massoulié, J., and Tsim, K. W. (2010) *J. Biol. Chem.* **285,** 27265–27278
22. Choi, R. C., Leung, P. W., Dong, T. T., Wan, D. C., and Tsim, K. W. (1996) *Neurosci. Lett.* **217,** 165–168
23. Ellman, G. L., Courtney, K. D., Andres, V., Jr., and Feather-Stone, R. M. (1961) *Biochem. Pharmacol.* **7,** 88–95
24. Santos, S. C., Vala, I., Miguel, C., Barata, J. T., Garção, P., Agostinho, P., Mendes, M., Coelho, A. V., Calado, A., Oliveira, C. R., e Silva, J. M., and Saldanha, C. (2007) *J. Biol. Chem.* **282,** 25597–25603
25. Tung, E. K., Choi, R. C., Siow, N. L., Jiang, J. X., Ling, K. K., Simon, J.,

Barnard, E. A., and Tsim, K. W. (2004) *Mol. Pharmacol.* **66,** 794–806
26. Holden, P., and Horton, W. A. (2009) *BMC Res. Notes* **2,** 243
27. Marra, P., Maffucci, T., Daniele, T., Tullio, G. D., Ikehara, Y., Chan, E. K., Luini, A., Beznoussenko, G., Mironov, A., and De Matteis, M. A. (2001) *Nat. Cell Biol.* **3,** 1101–1113
28. Meyer-Schaller, N., Chou, Y. C., Sumara, I., Martin, D. D., Kurz, T., Katheder, N., Hofmann, K., Berthiaume, L. G., Sicheri, F., and Peter, M. (2009) *Proc. Natl. Acad. Sci. U.S.A.* **106,** 12365–12370
29. Dobbertin, A., Hrabovska, A., Dembele, K., Camp, S., Taylor, P., Krejci, E., and Bernard, V. (2009) *J. Neurosci.* **29,** 4519–4530
30. Sussman, J. L., Harel, M., Frolow, F., Oefner, C., Goldman, A., Toker, L., and Silman, I. (1991) *Science* **253,** 872–879
31. Morel, N., Leroy, J., Ayon, A., Massoulié, J., and Bon, S. (2001) *J. Biol. Chem.* **276,** 37379–37389
32. Liang, D., Blouet, J. P., Borrega, F., Bon, S., and Massoulié, J. (2009) *FEBS J.* **276,** 94–108
33. Noureddine, H., Schmitt, C., Liu, W., Garbay, C., Massoulié, J., and Bon, S. (2007) *J. Biol. Chem.* **282,** 3487–3497
34. Palade, G. (1975) *Science* **189,** 347–358
35. Luzikov, V. N. (2002) *Biochemistry* **67,** 171–183
36. Rotundo, R. L. (1988) *J. Biol. Chem.* **263,** 19398–19406
37. Rotundo, R. L., Thomas, K., Porter-Jordan, K., Benson, R. J., Fernandez-Valle, C., and Fine, R. E. (1989) *J. Biol. Chem.* **264,** 3146–3152
38. Ruiz, C. A., and Rotundo, R. L. (2009) *J. Biol. Chem.* **284,** 21488–21495
39. Chatel, J. M., Grassi, J., Frobert, Y., Massoulié, J., and Vallette, F. M. (1993) *Proc. Natl. Acad. Sci. U.S.A.* **90,** 2476–2480
40. Choi, R. C., Yung, L. Y., Dong, T. T., Wan, D. C., Wong, Y. H., and Tsim, K. W. (1998) *J. Neurochem.* **71,** 152–160
41. Choi, R. C., Siow, N. L., Zhu, S. Q., Wan, D. C., Wong, Y. H., and Tsim, K. W. (2001) *Mol. Cell. Neurosci.* **17,** 732–745